Influence of Electrode Gas Flow Rate and Electrolyte Composition on Thermoelectric Power in Molten Carbonate Thermocell

S. Kandhasamy[a], L. Calandrino[b], O.S. Burheim[c], A. Solheim[d], S. Kjelstrup[e], and G.M. Haarberg[a]

[a] Department of Materials Technology and Engineering, Norwegian University of Science and Technology (NTNU), Trondheim, Norway
[b] Department of Mechanical and Industrial Engineering, University of Brescia, Brescia, Italy
[c] Department of Electrical Engineering and Renewable Energy, NTNU, Trondheim, Norway
[d] SINTEF Materials and Chemistry, SINTEF, Trondheim, Norway
[e] Department of Chemistry, NTNU, Trondheim, Norway

A thermocell (thermo-electrochemical cell) is an electrochemical system with two identical electrodes placed at different temperatures in an electrolyte solution. Ion transport between the electrodes due to the temperature gradient leads to thermoelectric power. These systems represent a promising pathway to utilize heat as a power source. A possible thermo-electrochemical cell with molten carbonate electrolyte and gas electrodes has been reported (1,2). The change in Seebeck coefficient (thermoelectric power) with electrode materials, electrode gas mixture, electrolyte composition and electrolyte support materials was studied (1). The addition of support material (solid oxide) in the molten carbonate electrolyte, may reduce the thermal conductivity and maintain the temperature gradient between the electrodes. Thermal boundary layers may arise due to the electrode gas flow rate; slow flow rate was preferred in the previous studies. In this study, the system is further studied to find an optimal ratio of electrolyte and support material, as well as electrode gas flow rate. The thermoelectric power is measured with various ratios of ($(Li,Na)_2CO_3$) molten carbonate mixed with solid oxide (MgO) in the electrolyte mixture and also with varying gas flow rates at the electrode-electrolyte interface.

Introduction

Thermoelectric cells converting heat into electricity are well known from the discovery of the Seebeck effect in 1821 (3). Thermoelectric power was demonstrated with aqueous thermogalvanic cells. However, because of the low efficiency due to high thermal conductivity of water and its low operating temperature semiconductors were preferred (4). Industrial metal production is associated with high energy consumption and high CO_2 emissions. Also, the energy efficiency is low as large amounts of heat are produced by irreversible losses. Thermoelectric converters based on semiconductor materials may be

used to generate electricity from the waste heat that is produced in such industries. Seebeck coefficients of the order of 0.8 mV/K are typical (5). The use of an ion conducting electrolyte and gas electrodes offers possibilities of achieving much higher Seebeck coefficients. Even though the aqueous thermocell has the drawbacks as stated above, it delivers higher Seebeck coefficients than semiconductor thermoelectric cells (6–8). Alternative electrolytes such as ionic liquids and molten salts (4,9) offer possibilities of high stable operating temperature and larger Seebeck coefficients than semiconductor thermoelectric materials (10). Experimental studies of electrochemical cells with molten carbonate electrolyte and CO_2/O_2 gas electrodes have been reported in our previous work where Seebeck coefficients in the range of 1.25 mV/K at a cell temperature of 750 °C were obtained (1).

The aim of these studies is to develop a thermoelectric cell with molten carbonate based electrolytes with symmetrical gas electrodes to utilize waste heat from metal production industries. The use of non-critical and non-poisonous materials and the prospective high thermoelectric efficiency, as well as the availability of CO_2 gas, may be advantageous compared to semiconductor thermoelectric cells. The so-called "figure of merit" is related to the thermoelectric generation efficiency, and it increases with a high Seebeck coefficient, a low thermal conductivity and a low electrical resistivity (4). A thermocell is an electrochemical system with two identical electrodes placed at different temperature in an electrolyte solution. Thermal diffusion in the electrolyte is set up due to the temperature gradient between the electrodes. A steady state condition, which is related to the Soret equilibrium, is achieved after a certain time. Seebeck coefficients are determined by measuring the steady state potential when no current is passing through the cell.

In the present work a solid phase of MgO is added to the electrolyte in order to improve the thermoelectric properties of the cell. The use of solid MgO in molten carbonate was first reported by Jacobsen and Broers (7). MgO has a very low solubility in the molten carbonate electrolyte, and MgO particles will be dispersed in the molten salt. The presence of a solid phase may reduce the heat conductivity of the electrolyte. A gas mixture of CO_2/O_2 is introduced to the electrodes to obtain electrodes reversible to the carbonate ion. The content of the solid MgO phase and the flow rate of electrode gas may influence the thermoelectric potential. These parameters were not systematically investigated before (1,2,7). Therefore, these parameters were investigated in the present work.

Experimental

Lithium carbonate (Li_2CO_3), sodium carbonate (Na_2CO_3) and magnesium oxide (MgO) were purchased from Sigma-Aldrich with purity > 99 %. Pre-made electrode gas mixtures containing 34% oxygen mixed with carbon dioxide were obtained from AGA, Norway. Gold sheet and wire for the electrodes and wires of platinum, platinum with 10% Rhodium for thermocouple fabrication were obtained from K.A. Rasmussen, Norway. Alumina tubes with one center bore of diameter 2.3 mm and four other bores with 0.75 mm diameter and a tubular crucible were obtained from MTC Haldenwanger, Germany. The flow rate of electrode gas supplied through the ceramic tubes was controlled by a pair of Brooks instrument Sho-Rate meters with ± 5% accuracy, both the

scale reading and appropriate flow rate conversion for the gas used, is shown in Table 1. The temperature of the electrodes and the cell potential were recorded by Agilent, 34972A data acquisition unit.

Thermo-electrochemical cell was constructed in a standard laboratory vertical tubular furnace (Figure 1). The cell consists of an Al_2O_3 tubular crucible, with two electrodes immersed in a molten carbonate electrolyte. In each alumina tube, the gold wire was inserted into the center bore (diameter 2.3 mm) of a 5-bore Al_2O_3 tube and the gold sheet was point-welded to the wire. The thermocouple (Pt-Pt10%Rh) was inserted into two of the other holes (diameter 0.75 mm) and the junction was positioned as near as possible to the gold sheet. CO_2/O_2 gas was supplied through the bores of the ceramic tube. The ratio of Li_2CO_3 and Na_2CO_3 eutectic mixture and dispersed solid MgO for electrolyte mixture and the CO_2/O_2 gas flow rate at the electrode/electrolyte interface are listed in Table I for different cells.

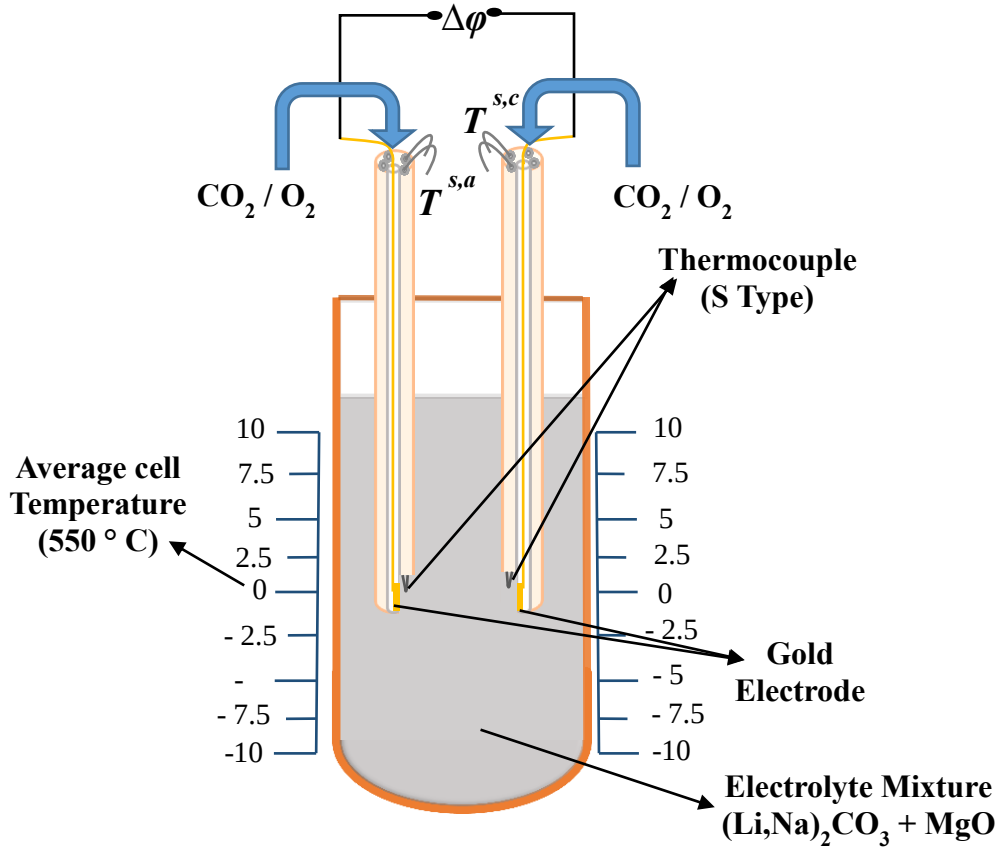

Figure 1. Cross sectional view of the thermo-electrochemical cell with reference scale for positioning the electrode to create the required temperature gradient. (Electrode positions for ΔT of 20 °C was $T^{s,a}$ and $T^{s,c}$ at 10 and -10 position respectively, vice versa for ΔT of -20 °C)

The electrochemical cell with gas electrodes, reversible to the carbonate ion, held at different temperatures can be represented as:

$$\text{Au } (T^{s,a}) \mid CO_2 \text{ (g)} , O_2 \text{ (g)} \mid (\text{Li, Na})_2CO_3 \text{ (l)} , \text{MgO (s)} \mid CO_2 \text{ (g)} , O_2 \text{ (g)} \mid \text{Au } (T^{s,c})$$

The electrochemical reaction at the left-hand side electrode is:

$$\frac{1}{2}\ CO_3^{2-}\ (l) \rightarrow \frac{1}{2}\ CO_2\ (g) + \frac{1}{4}\ O_2\ (g) + \ e^- \qquad [1]$$

The reverse reaction takes place at the right-hand side. The Seebeck coefficient for the cell with uniform (homogeneous electrolyte) melt composition (short time) is:

$$\alpha_S = \left(\frac{\Delta\varphi}{(T^{s,c} - T^{s,a})}\right)_{j=0,t=0}$$

$$= -\frac{1}{F}\left[\frac{1}{2}\ S_{CO_2} + \frac{1}{4}\ S_{O_2} + S_e^* - \frac{1}{2}\ S_{CO_3^{2-}}^* + \left(\frac{t_2}{x_2} - \frac{t_1}{x_1}\right)\frac{q^*}{T}\right] \qquad [2]$$

where, S_j is the entropy of component j at average temperature of the electrodes T and pressure p_j. The terms S_e^* and $S_{CO_3^{2-}}^*$ are the transported entropy of the electron and carbonate ion respectively. The entropies and the transported entropies are generally functions of temperature. Then t_1, t_2 are the transference coefficient and x_1, x_2 are the mole fractions of Li_2CO_3 and M_2CO_3. The ratio $\frac{q^*}{T}$ may be interpreted in terms of enthalpy changes across the layer. A detailed theoretical derivation of the equation based on non-equilibrium thermodynamics is explained in our previous work (1,2).

TABLE I. Electrode gas flow rate and MgO to carbonate ratio used in the experiments.

Cell Label		CO_2 / O_2 Flow rate		Weight %		Volume %	
		Scale Reading (NML/M)	Scale Conversion (ml/min)	MgO	Eutectic Mixture Li_2CO_3 + Na_2CO_3	MgO	Eutectic Mixture Li_2CO_3 + Na_2CO_3
Varying Electrode Gas Flow Rate	A	40	14.7	55	45	44.3	55.7
	B	50	16.1				
	C	60	18.6				
	D	70	21.0				
	E	80	23.4				
Differential Ratio of MgO in Electrolyte	D	70	21.0	55	45	44.3	55.7
	F			65	35	54.7	45.3
	G			75	25	66.1	33.9
	H			85	15	78.7	21.3

A temperature difference (ΔT) was established between the electrodes by positioning them at different heights in the crucible. The average cell temperature was kept at 550 °C and the temperature difference was always smaller than 20 °C. The electromotive force between the electrodes was measured as a function of the temperature difference, after an equilibration period of 10-20 min and a measurement with a new temperature difference was done. Recordings were made over time at a certain temperature difference to make sure that the situation was stable for a long time. The electrolyte preparation and cell measurements were performed using the same procedure as in our previous reports (1,2).

The phase analysis of the electrolyte mixture was carried out before and after thermo-electrochemical cell measurements, using Bruker-D8 ADVANCE X-ray diffraction (XRD) with CuKα radiation (λ = 1.5406 Å). The elemental composition was also

determined on the same samples by Energy Dispersive Spectroscopy (EDS) using an Oxford instrument Aztec EDS system attached to a Hitachi S-3400N Scanning Electron Microscopy (SEM). The front beryllium window in the detector absorbs low-energy X-rays. Thus, EDS cannot detect the presence of elements with atomic number less than 5 which includes Li, while all other possible elements in the electrolyte mixture were detected.

Results and discussion

Influence of gas flow rate on the Seebeck coefficient

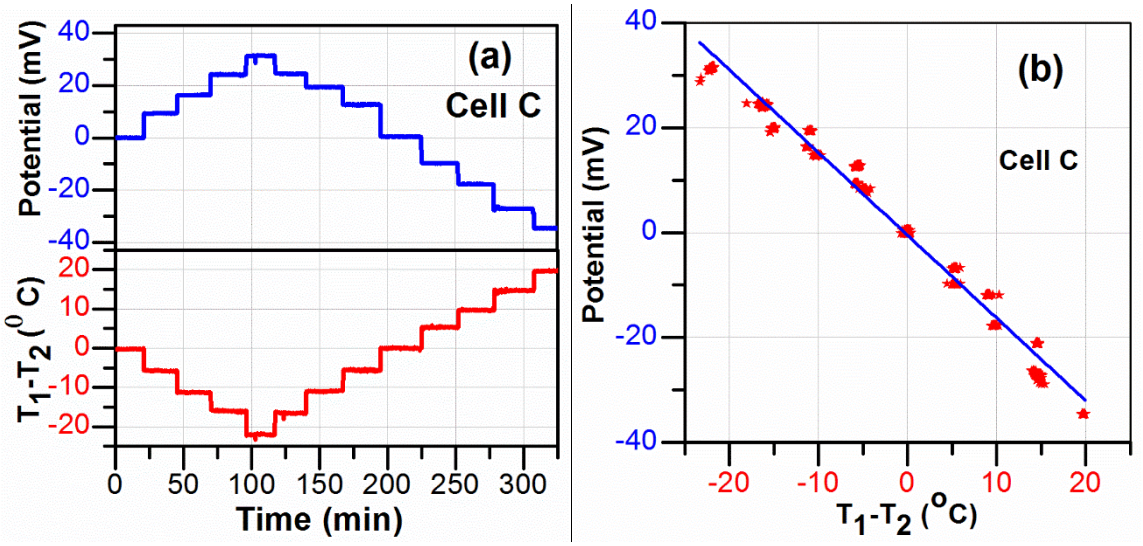

Figure 2. (a) The measured potential and temperature difference and, (b) Seebeck coefficient plot for cell C with electrode gas flow rate of 18.6 ml/min.

TABLE II. Seebeck coefficient of the cells with varying electrode gas flow rate.

Cell Label	CO_2 / O_2 Flow rate (ml/min)	Volume %		Seebeck Coefficient (mV/ K)	
		MgO	Eutectic Mixture Li_2CO_3 + Na_2CO_3	Slope	Standard Error
A	14.7			-1.1	0.003
B	16.1			-1.2	0.003
C	18.6	44.3	55.7	-1.6	0.003
D	21.0			-1.7	0.005
E	23.4			-1.0	0.003

Measured steady state thermoelectric potential and the respective temperature difference between the electrodes were recorded as a function of time as shown in Figure 2(a). The negative temperature steps show a positive increase in potential and a negative potential for positive temperature change was observed (11). Similarly, the thermoelectric potential and temperature difference between the electrodes were recorded for all the cells with an average operating temperature of 550 °C. The recorded potential is plotted against the respective temperature difference, to calculate the average Seebeck coefficient from the slope of the linear fit (Figure 2(b)). The determined Seebeck coefficients are similar to previously reported values (1, 2). However, it was found that the increase in gas flow rate caused an increase in the Seebeck coefficient from cell A (1.1 mV/K) to D

(1.7 mV/K), as shown in Table II. The Seebeck coefficient was reduced to 1 mV/K by further increasing the gas flow beyond the rate in cell D.

Steady state and high gas flow rate

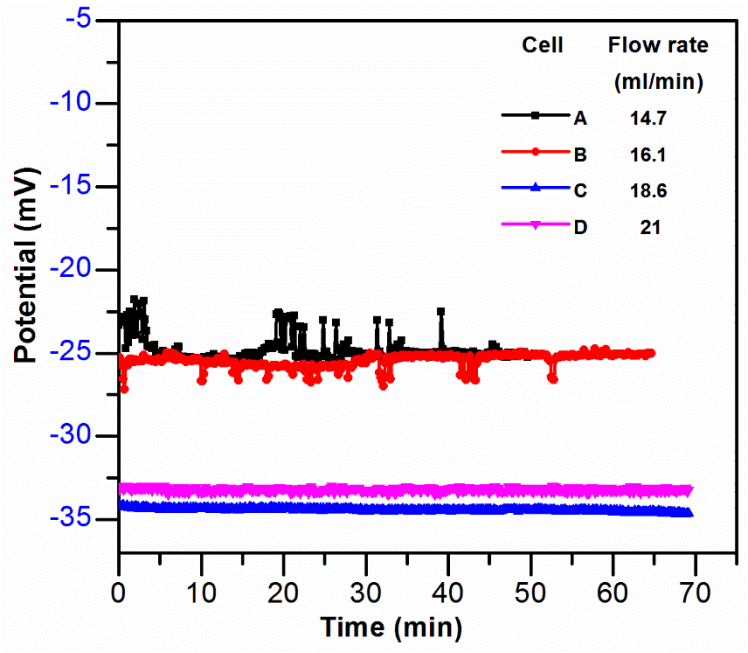

Figure 3. Measured potential versus time for electrode temperature difference of 20 °C with varying electrode gas flow rate (Cell A-D).

The thermoelectric potential recorded in all the experiments was the value measured at steady state. The potential difference between the electrodes immediately after establishing the temperature difference is known as initial thermoelectric potential. The steady state condition is established after a long time; 20 – 30 min, sometimes even longer (12–14). In cell A and B with low flow rate, the initial thermoelectric potential for the change in electrode positions was attained as soon as the temperate gradient was stabilized. This was followed by a change to lower potentials and a shift toward higher values before reaching a stable potential (15, 13). The time to establish the Soret equilibrium is mainly dependent on the ion transport on response to the temperature gradient. The time was estimated by Kang et al (1) to 70 hrs, without detailed knowledge of the interdiffusion coefficient. On this basis, the authors related their Seebeck coefficient to the initial state (t = 0). The gas flow rate was not precisely recorded in their experiments, however. Also, we do not know if Soret equilibrium can be reached. However, a further increase in gas flow rate in cell C and D, prevents the development of the concentration gradient. This caused the steady state condition to be established immediately, whereas in cell A and B steady state was observed after 20 – 30 min. Data in the plot (cell C and D in Figure 3) are shown only for up to 70 min of the measurements, which was actually measured for more than 15 h and showed less than 0.5 % deviation from the initial value. Thus the gas flow rate of ~21 ml/min limits the growth of concentration gradient and circulates the ions in the electrolyte to maintain homogeneity, which keeps the thermoelectric potential generation stable for a long time (16).

Solid oxide to molten carbonates ratio

The thermo-electrochemical cell with gas flow rate of 20 ml/min and the same average temperature of 550 °C was used to study the cells with different contents of MgO in the electrolyte mixture for comparison (Table I). The electrolyte is not compacted, just filled as a free powder in the crucible. This free packing provides the flexiblity in distributing the molten salt through the solid phase. This system offers the high ion mobility with low heat conductivity for possible enhanced thermoelectric conversion (17). These cells (D, F & G) results in the same range of Seebeck coefficients (1.7 mV/K), even with different ratios of MgO to carbonates (Table III). The increase in the content of MgO beyond the ratio in cell G leads to a low ratio of melt to solid and affects the establishment of ion transport matrix in the electrolyte. In the cell H (Figure 4(b)), the potential decreased as the temperature gradient increased (increase in electrode separation distance) above ± 5 °C. Even though the high solid content provides a low heat conductivity, the low melt concentration in the electrolyte is not able to produce a well-defined Seebeck coefficient. Conditions in the melt at no longer well defined.

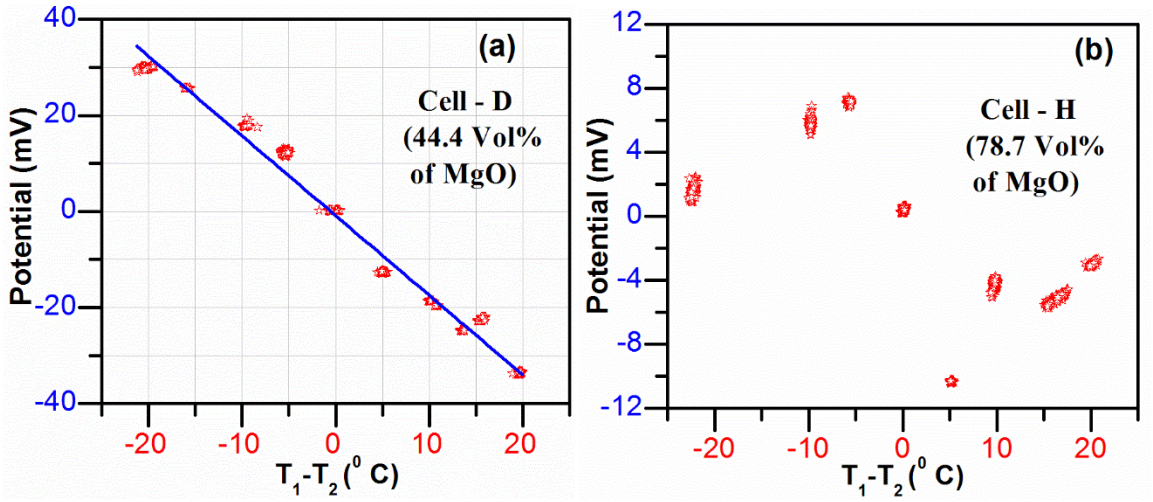

Figure 4. (a) Seebeck coefficient plot for cell D, and (b) Measured potential versus temperature difference in the cell H.

TABLE III. Seebeck coefficient of the cells with different ratio MgO in electrolyte.

Cell Label	CO_2 / O_2 Flow rate (ml/min)	Volume %		Seebeck Coefficient (mV/K)	
		MgO	Eutectic Mixture $Li_2CO_3 + Na_2CO_3$	Slope	Standard Error
D		44.3	55.7	-1.7	0.005
F	21.0	54.7	45.3	-1.7	0.004
G		66.1	33.9	-1.7	0.005

Results from X-ray diffraction analysis of the electrolyte samples collected from the various regions of the cells (D and G) after performing thermo-electrochemical measurements are shown in Figure 5(a & b). No significant changes in peak positions were observed for samples from different regions, confirming the homogeneity of the electrolyte mixture throughout the cell. In Figure 5(a & c) the absence of additional peaks before and after the thermo-electrochemical reaction endorses no impurities formation. Therefore, electrolyte decomposition or carbonate reacting with MgO does not happen in

the cell (18). Also, these indistinguishable XRD patterns for the samples from different regions, confirm the homogeneity of the electrolyte throughout the experiment. The gas flow rate of 21 ml/min avoids the expansion of concentration gradients in the electrolyte and helps in maintaining the homogeneity. No significant change in the peaks intensity ratio of MgO (Figure 5(a & c)) before and after cell reaction was observed, which suggests that MgO is a solid phase throughout the experiment. The carbonates undergo a phase change from solid to melt and solidification afterwards. A poor crystallinity is attained during re-solidification in the presence of insulating solid oxide, which shows a significant reduction in peak intensity corresponding to molten carbonate.

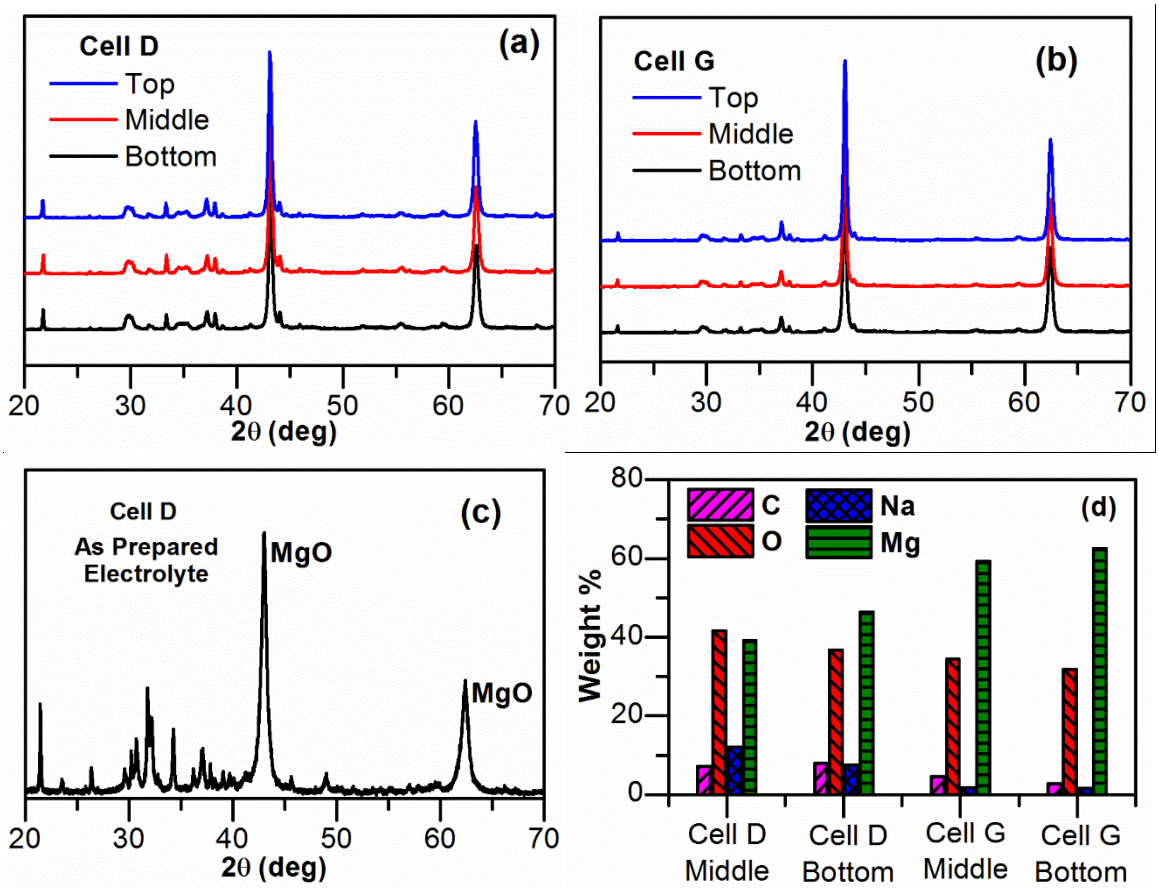

Figure 5. X-ray diffraction patterns for the electrolyte mixer after (a,b) and before (c) thermo-electrochemical measurement. (d) EDS elemental analysis of the electrolyte after thermo-electrochemical measurement.

EDS analysis was performed on the used electrolyte to acquire more accurate information about elemental distribution than XRD analysis could reveal. Figure 5(d) is plotted with an average value of the analysis performed at least in two different locations in each sample. Observations after the experiments indicate that there was ~ 3 - 5 wt % higher concentration of MgO at the bottom of both the cells, which may be due to settling of the solid phase in the melt. Therefore, the electrolyte is assumed to be homogeneously prepared and the homogeneity is maintained throughout the cell operation by employing the moderate gas bubbling rate of 21 ml/min.

Conclusions

The thermoelectric potential for the molten carbonate thermocell was measured with different flow rates of electrode gas and solid oxide ratios in the electrolyte. Seebeck coefficients on the order of 1.66 mV/K were obtained. The rate of the gas flow was found to influence the Seebeck coefficient. The influence of the gas flow rate in maintaining the electrolyte homogeneity was evidenced by XRD and EDS studies.

Acknowledgment

The authors wish to acknowledge the Research Council of Norway for financial support in the research project "Sustainable and Energy Efficient Electrochemical Production and Refining of Metals (SUPREME)".

References

1. X. Kang, M. T. Børset, O. S. Burheim, G. M. Haarberg, Q. Xu and S. Kjelstrup, *Electrochim. Acta* **182,** 342 (2015).
2. M. T. Børset, X. Kang, O. S. Burheim, G. M. Haarberg, Q. Xu and S. Kjelstrup, *Electrochim. Acta* **182,** 699 (2015).
3. E. Bouty, *J. Phys. Theor. Appl* **9,** 229 (1880).
4. T. I. Quickenden and Y. Mua, *J. Electrochem. Soc.* **142,** 3985 (1995).
5. M. Hamid Elsheikh, D. A. Shnawah, M. F. M. Sabri, S. B. M. Said, M. Haji Hassan, M. B. Ali Bashir and M. Mohamad, *Renew. Sustain. Energy Rev.* **30,** 337 (2014).
6. K. Cornwell, *J. Phys. D. Appl. Phys.* **1,** 173 (1968).
7. T. Jacobsen and G. H. J. Broers, *J. Electrochem. Soc.* **124,** 207 (1977).
8. B. Burrows, *J. Electrochem. Soc.* **123,** 154 (1976).
9. Y. Ito and T. Nohira, *Electrochim. Acta* **45,** 2611 (2000).
10. Y. V. Kuzminskii, V. A. Zasukha, and G. Y. Kuzminskaya, *J. Power Sources* **52,** 231 (1994).
11. M. Bonetti, S. Nakamae, M. Roger, and P. Guenoun, *J. Chem. Phys.* **134,** 1 (2011).
12. K. Sasaki and S. Nagaura, *Bull. Chem. Soc. Jpn.* **31,** 498 (1958).
13. M. Bonetti, S. Nakamae, B. T. Huang, T. J. Salez, C. C. Wiertel-Gasquet, and M. Roger, *J. Chem. Phys.* **142,** 1 (2015).
14. T. Ikeshoji, *Bulletin of the Chemical Society of Japan* **60,** 1505 (1987).
15. J. N. Agar and W. G. Breck, *Nature* **175,** 298 (1955).
16. R. S. Goncalves and T. Ikeshoji, *J. Braz. Chem. Soc.* **3,** 98 (1992).
17. J. Josserand, V. Devaud, G. Lagger, H. Jensen, and H. H. Girault, *J. Electroanal. Chem.* **565,** 65 (2004).
18. M. Mizuhata, Y. Harada, G. Cha, A. B. Béléké and S. Deki, *J. Electrochem. Soc.* **151,** E179 (2004).